El Niño-Southern Oscillation Feedback in JMA's Seasonal Forecast Model

Satoko Matsueda and Yuhei Takaya

Climate Prediction Division, Japan Meteorological Agency

(E-mail: matsueda@met.kishou.go.jp)

Introduction

It is important for seasonal prediction to represent El Niño-Southern Oscillation (ENSO) appropriately in an atmosphere-ocean coupled global circulation model (CGCM). ENSO forecast skill in JMA's operational seasonal forecast model (JMA/MRI-CGCM) is comparable to that of models used in other major centers. However, the amplitude, frequency and spatial pattern of ENSO as predicted by the JMA model differ from the results of actual ENSO analysis. ENSO representation among CGCMs is diverse, and it has been suggested that atmospheric models play a dominant role in determining ENSO amplitude and frequency in CGCMs (Guilyardi et al. 2009). In this study, two types of atmospheric feedback (ENSO feedback) were diagnosed with reference to the method proposed by Lloyd et al. (2009).

Data

Single-member forecasts in a set of hindcasts were analyzed using JMA's CGCM with (CGCM_FLAD) and without flux adjustment (CGCM_NFLAD). Forecasts were initialized twice a month for CGCM_FLAD and once a month for CGCM_NFLAD for the period 1979 – 2008. An AMIP-type run with JMA's CGCM was also used for the period 1979 – 2010, a quasi-coupled data assimilation system data set (MOVE-C; Fujii et al. 2009) was used for the period 1979 – 2009, and JRA-55 reanalysis data (Ebita et al. 2011) were used for the period 1980 – 1999. The monthly mean fields of all variables were analyzed.

Diagnosis method for ENSO feedback

Lloyd et al. (2009) diagnosed two types of atmospheric feedback (dynamical and total heat flux) that have a dominant influence on ENSO. Dynamical feedback is represented as follows:

$$\tau_x{}' = \mu T'.$$

This is known as Bjerknes feedback (Bjerknes 1969) –
a positive type in which a positive (negative) sea surface temperature (SST) anomaly (T') induces a westerly (easterly) wind stress anomaly ($\tau_x{}'$), enhancing a positive (negative) SST anomaly.

The total heat flux feedback is represented as follows:

$$Q' = \alpha T'.$$

This is considered to be a negative type in which a positive (negative) SST anomaly (T') increases (reduces) the total heat flux (Q), resulting in SST anomaly decay. Total heat flux feedback (α) consists of contributions from latent heat flux (LH), sensible heat flux (SH), short-wave radiative flux (SW) and long-wave radiative flux (LW).

Remote dynamical feedback μ, local dynamical feedback μ_L and local heat flux feedback α were calculated with reference to the method proposed by Lloyd et al. (2009). Results averaged for 1 – 7 forecast months were shown as CGCM diagnostics.

Diagnosis results

Figure 1 shows ENSO feedback estimated from each type of data. The dynamical (μ and μ_L) and total heat (α) feedback in CGCMs has the same sign as JRA-55 reanalysis results and is reasonable compared to that of CMIP3 models (Lloyd et al. 2009). However, the feedback is underestimated in CGCMs compared to JRA-55. For the AMIP run, μ and α are closer to JRA-55. Similar results were obtained from CMIP3 models (Lloyd et al. 2009 and Lloyd et al. 2011). MOVE-C also underestimates μ and α. Lloyd et al. (2009) suggested that α is related to ENSO amplitude and influences ENSO representation in coupled models. Figure 2 shows the values of four heat/radiative flux feedback components (α_{LH}, α_{SW}, α_{LW}, and α_{SH}). For all data, α_{LH} and α_{SW} are dominant, and α_{LH} is well represented. However the value of α_{SW} depends on the models, and can be seen as a significant factor contributing to errors in α

(Lloyd 2009). The amplitude of α_{SW} for the AMIP run is larger than that for CGCMs and similar to that for JRA-55. These characteristics are also seen with CMIP3 models (Lloyd et al. 2011). The spatial distribution of α_{SW} is shown in Figure 3. Negative feedback of α_{SW} in the NINO.3 region related to large-scale convective activity is reproduced by all models but is underestimated by CGCMs and MOVE-C compared to the results of JRA-55 and the AMIP run. Positive feedback of α_{SW} off the coast of Peru (in a region of large-scale subsidence) is overestimated by CGCMs compared to the results of JRA-55, and by most CMIP3 models (Lloyd et al. 2012). The underestimation of precipitation anomalies during ENSO events and poor representation of clouds over the tropics in models can be considered as possible reasons for this. The diagnostics presented here offer a way to clarify and assess the representation of ENSO feedback in atmospheric models.

References

Ebita, A., S. Kobayashi, Y. Ota, M. Moriya, R. Kumabe, K. Onogi, Y. Harada, S. Yasui, K. Miyaoka, K. Takahashi, H. Kamahori, C. Kobayashi, H. Endo, M. Soma, Y. Oikawa and T. Ishimizu, 2011: The Japanese 55-year Reanalysis "JRA-55": An Interim Report. *SOLA*, **7**, 149 – 152.

Fujii, Y., T. Nakaegawa, S. Matsumoto, T. Yasuda, G. Yamanaka and M. Kamachi, 2009: Coupled climate simulation by constraining ocean fields in a coupled model with ocean data. *J. Climate*, **22**, 5541 – 5557.

Guilyardi, E. et al., 2009: Understanding El Niño in ocean-atmosphere general circulation models: Progress and challenges. *Bull. Amer. Meteor. Soc.*, **90**, 325 – 340.

Lloyd, J., E. Guilyardi, H. Weller and J. Slingo, 2009: The role of atmosphere feedbacks during ENSO in the CMIP3 models. *Atmos. Sci. Lett.*, **10**, 170 – 176.

Lloyd, J., E. Guilyardi, H. Weller, and J. Slingo, 2011: The role of atmosphere feedbacks during ENSO in the CMIP3 models. Part II: Using AMIP runs to understand the heat flux feedback mechanisms. *Climate Dyn.*, **37**, 1271 – 1292.

Lloyd, J., E. Guilyardi, H. Weller, 2012: The role of atmosphere feedbacks during ENSO in the CMIP3 Models. Part III: the shortwave flux feedback. *J. Climate*, **25**, 4275 – 4293.
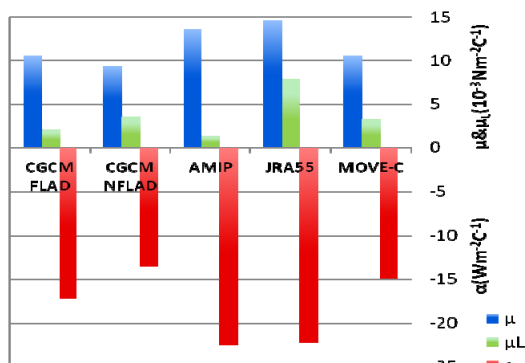
Figure 1   Average annual NINO.4 μ (blue), NINO.3 μL (green) and NINO.4 α(red) values for CGCM_FLAD, CGCM_NFLAD, AMIP run, JRA-55 and MOVE-C
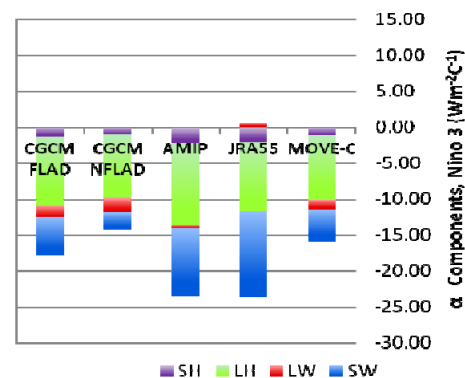

Figure 2   Average annual α components: α_{SH}(purple), α_{LH}(green), α_{LW}(red) and α_{SW}(blue) for CGCM_FLAD, CGCM_NFLAD, AMIP run, JRA-55 and MOVE-C
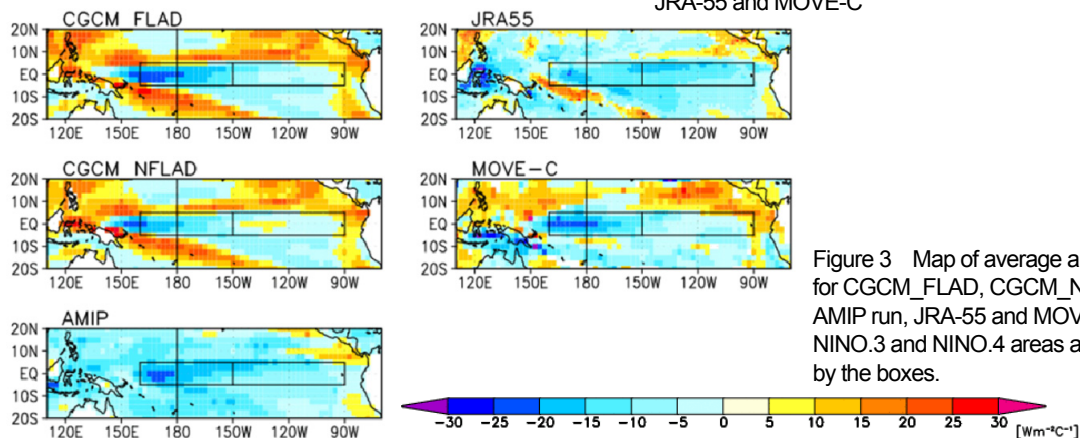

Figure 3   Map of average annual α_{SW}, for CGCM_FLAD, CGCM_NFLAD, AMIP run, JRA-55 and MOVE-C. The NINO.3 and NINO.4 areas are shown by the boxes.